










Coronary CT Angiography in the Cath Lab: Leveraging Artificial Intelligence to Plan and Guide Percutaneous Coronary Intervention

Hirofumi Ohashi,^{1,2} Frédéric Bouisset ^{1,3} Dimitri Buytaert ¹ Ruiko Seki ¹ Jeroen Sonck ¹ Koshiro Sakai,^{1,4} Marta Belmonte ^{1,5} Pieter Kitslaar ⁶ Adam Updegrave,⁷ Tetsuya Amano ² Daniele Andreini ^{8,9} Bernard De Bruyne^{1,10} and Carlos Collet ¹

1. Cardiovascular Center OLV, Aalst, Belgium; 2. Department of Cardiology, Aichi Medical University, Aichi, Japan; 3. Department of Cardiology, Toulouse University Hospital, Toulouse, France; 4. Department of Cardiology, Showa University Hospital, Tokyo, Japan; 5. Department of Advanced Biomedical Sciences, University Federico II, Naples, Italy; 6. Medis Medical Imaging Systems, Leiden, the Netherlands; 7. HeartFlow Inc., Redwood City, CA, US; 8. Division of Cardiology and Cardiac Imaging, IRCCS Ospedale Galeazzi – Sant'Ambrogio, Milan, Italy; 9. Department of Biomedical and Clinical Sciences, University of Milan, Milan, Italy; 10. Department of Cardiology, University Hospital of Lausanne, Lausanne, Switzerland

Abstract

The role of coronary CT angiography for the diagnosis and risk stratification of coronary artery disease is well established. However, its potential beyond the diagnostic phase remains to be determined. The current review focuses on the insights that coronary CT angiography can provide when planning and performing percutaneous coronary interventions. We describe a novel approach incorporating anatomical and functional pre-procedural planning enhanced by artificial intelligence, computational physiology and online 3D CT guidance for percutaneous coronary interventions. This strategy allows the individualisation of patient selection, optimisation of the revascularisation strategy and effective use of resources.

Keywords

Coronary CT angiography, percutaneous coronary intervention, fractional flow reserve derived from CT, coronary artery disease, 3D CT-derived coronary geometry

Disclosure: MB has received research grants from the Cardiopath PhD programme. PK is an employee of Medis Medical Imaging Systems. AU is an employee of HeartFlow. DA has received research grants from GE Healthcare and Bracco. FB has received consultancy fees from Boston Scientific, B-Braun and Amgen. BDB has received consultancy fees from Boston Scientific and Abbott, and research grants from Coroventis Research, Pie Medical Imaging, Cathworks, Boston Scientific, Siemens, HeartFlow and Abbott Vascular. CC has received consultancy fees from HeartFlow, OpSens, Abbott Vascular and Philips Volcano, and research grants from Biosensor, Coroventis Research, Medis Medical Imaging, Pie Medical Imaging, CathWorks, Boston Scientific, Siemens, HeartFlow and Abbott Vascular. All other authors have no conflicts of interest to declare.

Consent: All patients have given written informed consent for use of their images.

Received: 18 April 2023 **Accepted:** 15 August 2023 **Citation:** *Interventional Cardiology* 2023;18:e26. **DOI:** <https://doi.org/10.15420/icr.2023.12>

Correspondence: Carlos Collet, Cardiovascular Center, Onze-Lieve-Vrouweziekenhuis, Moorselbaan 164, 9300, Aalst, Belgium. E: carloscollet@gmail.com

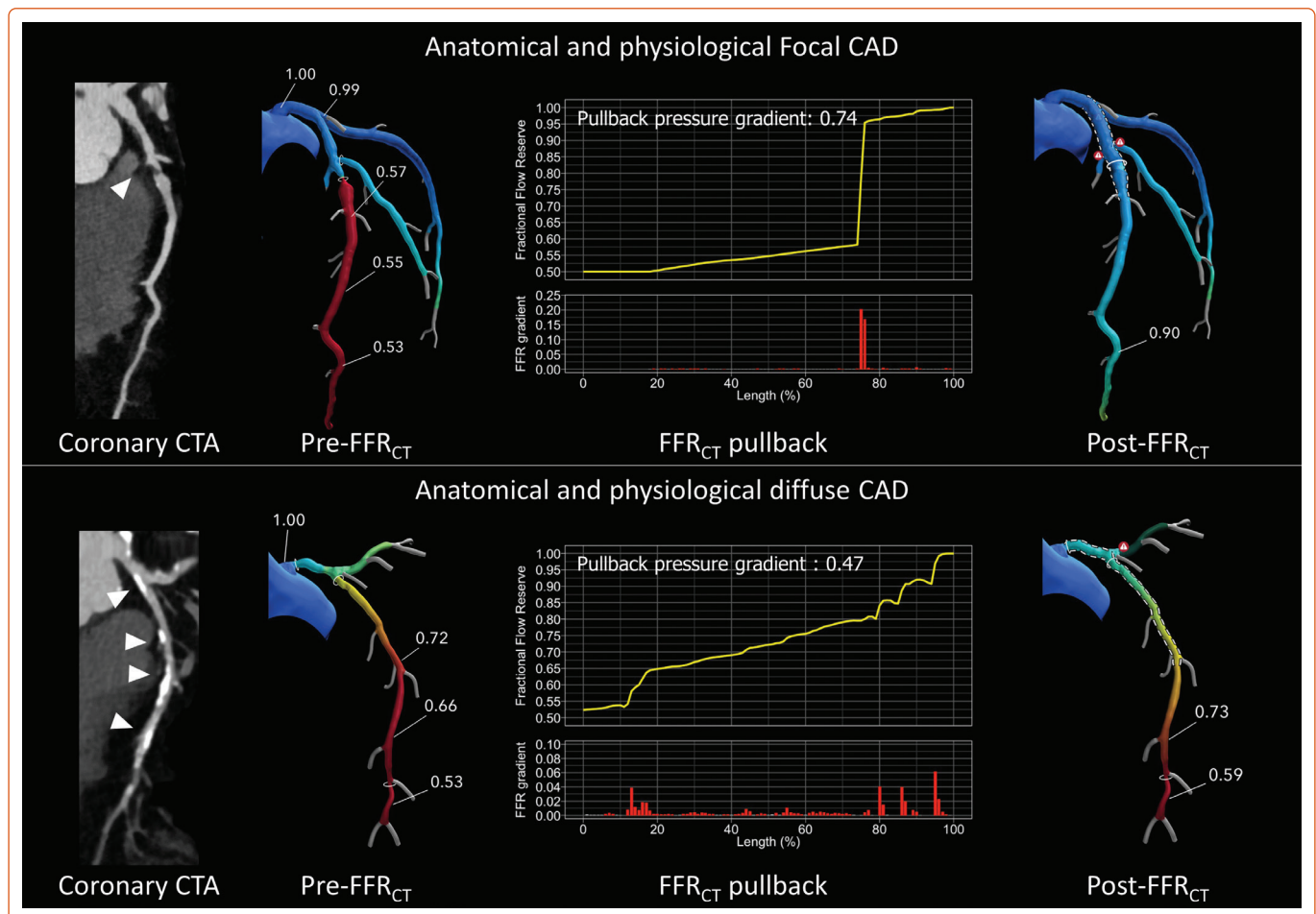
Open Access: This work is open access under the CC-BY-NC 4.0 License which allows users to copy, redistribute and make derivative works for non-commercial purposes, provided the original work is cited correctly.

Coronary CT angiography (CTA) is a well-established tool for diagnosing coronary artery disease (CAD). Coronary CTA also facilitates the assessment of a patient's risk based on plaque characteristics.¹ Current guidelines recommend using coronary CTA as the initial assessment for patients with chest pain.² Additionally, fractional flow reserve (FFR) can be estimated with conventional coronary CTA, providing a combined anatomical and functional evaluation in one test. FFR derived from CT (FFR_{CT}) technology also enables virtual percutaneous coronary intervention (PCI) and predicts the degree of functional revascularisation following PCI using the FFR_{CT} Planner.³ Studies and meta-analyses have linked the degree of functional revascularisation after PCI, measured by post-PCI FFR, to hard outcomes.⁴ This level of outcome prediction is unprecedented and could impact the CAD field, leading to improved patient outcomes. This review focuses on describing the basics and perspectives of coronary CTA analysis, emphasising the role of artificial intelligence in the planning and guidance of revascularisation procedures.

Risk Assessment Based on Coronary CT Angiography Before Revascularisation

Prior to considering revascularisation, coronary CTA effectively stratifies patients in terms of procedural outcomes. Procedural risk associated with PCI can be estimated based on disease complexity and the anatomical features of the lesion to be treated. Coronary CTA allows risk stratification according to disease extension (e.g. one-vessel disease, two-vessel disease, three-vessel disease or left main disease).⁵ Anatomically high-risk procedures can be defined by the type of lesion, disease affecting major bifurcations, calcification severity or the presence of total coronary occlusions. Moreover, lipidic plaque composition based on coronary CTA is associated with periprocedural injury, probably because of material embolisation to the coronary microcirculation. Peri-procedural MI has been shown to be higher in lesions with high-risk plaque characteristics.⁶ Lipid-rich plaque with the napkin ring sign and low-attenuation plaque has been linked to risk of a no-reflow during PCI.⁷⁻⁹ These high-risk plaque

Figure 1: Case Examples of Focal and Diffuse Coronary Artery Disease Detected by Coronary CT Angiography and Fractional Flow Reserve Derived From CT



A: This case shows a functional focal lesion in the mid-left anterior descending artery. The virtual pullback curve derived from FFR_{CT} shows a focal pressure drop of approximately 0.35 FFR_{CT} units related to the lesion (top centre) with a PPG of 0.74. After virtual PCI, the predicted FFR_{CT} was 0.90. B: This case shows functional diffuse CAD in a left anterior descending artery. The virtual pullback curve derived from FFR_{CT} shows diffuse pressure losses along the vessel length (bottom centre) with a PPG of 0.47. After virtual PCI, the predicted FFR_{CT} was 0.59. CAD = coronary artery disease; CTA = CT angiography; FFR = fractional flow reserve; FFR_{CT} = FFR derived from CT; PCI = percutaneous coronary intervention; PPG = pullback pressure gradient.

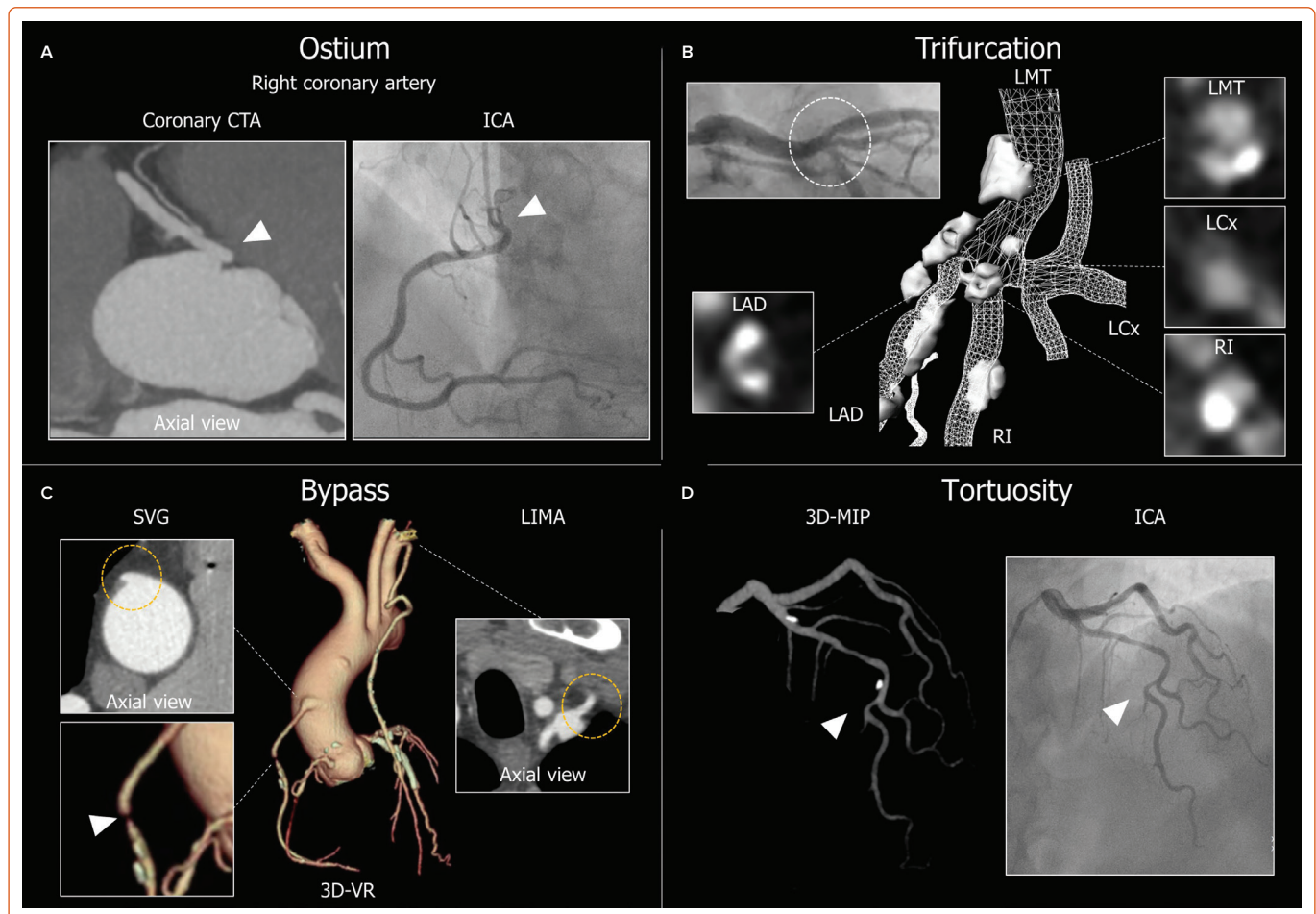
characteristics, e.g. positive remodelling and low-attenuation plaque, also carry a higher risk for spontaneous MI. To correctly identify these plaques, algorithms for vessel wall detection are being enriched by deep learning methods to provide measurements of plaque volume and composition that closely correlate with intravascular imaging.¹⁰ Artificial intelligence algorithms are increasingly being applied to coronary CTA to improve the efficiency, reproducibility and accuracy of image analysis.¹¹ These algorithms have proven to have an excellent capacity for predicting MI in patients with CAD. The next step is to apply these methods to pre-procedural stratification in patients considered for revascularisation. The availability of coronary CTA for stratification based on artificial intelligence may inform the best treatment strategy. Therefore, the risk of an intervention based on patient-specific information could be established, enhancing the decision-making process about revascularisation and allowing procedural planning.

Coronary Physiology Derived From Coronary CT Angiography

FFR_{CT} is calculated by applying computational fluid dynamics (CFD) to coronary geometries extracted from CTA. FFR_{CT} is then defined as the computed mean coronary pressure distal to a lesion divided by the mean pressure in the aorta under simulated maximal hyperaemia.³ The FFR_{CT} results are presented on a 3D model of the coronary arteries, and colour-

coded based on the FFR_{CT} value at each level. Nørgaard et al. demonstrated that the use of FFR_{CT} compared with a visual assessment alone, improved the diagnostic performance of the detection of haemodynamically significant lesions.¹² Furthermore, FFR_{CT} facilitates the assessment of the functional pattern of CAD, i.e. focal or diffuse, by providing longitudinal vessel information mimicking invasive pressure pullbacks.¹³ Identifying the functional CAD pattern beyond the distal FFR value alone not only influences the revascularisation strategy but also provides additional risk stratification for plaque rupture and MI.¹⁴ Moreover, the trans-lesional pressure gradient of FFR_{CT} (ΔFFR_{CT}) is an independent predictor of MI. Furthermore, the haemodynamic patterns of CAD are linked to the benefit of PCI in terms of angina relief. PCI restores epicardial conductance in cases of focal CAD, whereas blood flow improvement after PCI in cases of diffuse disease is significantly lower.¹⁵ The pattern of CAD, quantified by the pullback pressure gradient (PPG), has been associated with freedom from angina after PCI; residual angina is almost twice as common in patients with a low PPG (haemodynamic diffuse disease) compared with high PPG (focal disease).¹⁶ Thus, the addition of functional information derived from CTA enhances risk prediction at the lesion level while providing information on the clinical benefit of revascularisation in terms of angina relief. The FFR_{CT} technology leverages machine-learning-based techniques to segment the coronary geometry that is used for CFD as well as to

Figure 2: Representation of Information on Coronary Anatomy by Coronary CT Angiography



A: An RCA ostium. The left image shows the coronary CTA with axial images. The white arrow indicates the position of ostial RCA that have anterior take off. The right image shows the invasive coronary angiography showing a difficulty-selective catheterisation. The information of coronary ostium, adapted to the RCA take off allows a good catheterisation of the artery and consequently a good visualisation of the RCA; B: A left-main trifurcation into the LAD, RI and LCx branches. The top left image shows the ICA of the LCA. The centre image shows the 3D coronary tree with calcification. The coronary CTA cross-sectional images show the position of the ostia in the trifurcation; C: The coronary CTA in patients with CABG. The middle image shows the 3D VR of the coronary arteries and bypass grafts. The left top image shows the ostial SVG in axial image (orange circle), the right image shows the ostial LIMA in axial image (orange circle). The white arrow of the left bottom image indicates the severe stenosis in the middle of the SVG; D: The coronary tortuosity in the LAD. The left panel shows the 3D MIP of the coronary CTA. The right panel shows ICA in the LCA. CABG = coronary artery bypass grafting; CTA = CT angiography; ICA = invasive coronary angiography; LAD = left anterior descending artery; LCA = left coronary artery; LCx = left circumflex artery; LIMA = left internal mammary artery; MIP = maximum intensity projection; RCA = right coronary artery; RI = ramus intermedius; SVG = saphenous vein graft; VR = volume rendering.

segment plaque volumes and types. Moreover, machine-learning techniques can be applied to improve the accuracy of the FFR predictions using invasive data or by replacing the necessity of CFD. From a clinical perspective, the addition of reliable physiological information to coronary CTA improves cath lab efficiency by providing a complete physiological map without the need for a pressure wire.¹⁷ Two case examples of the application of the planner in cases of focal and diffuse CAD are shown in Figure 1.

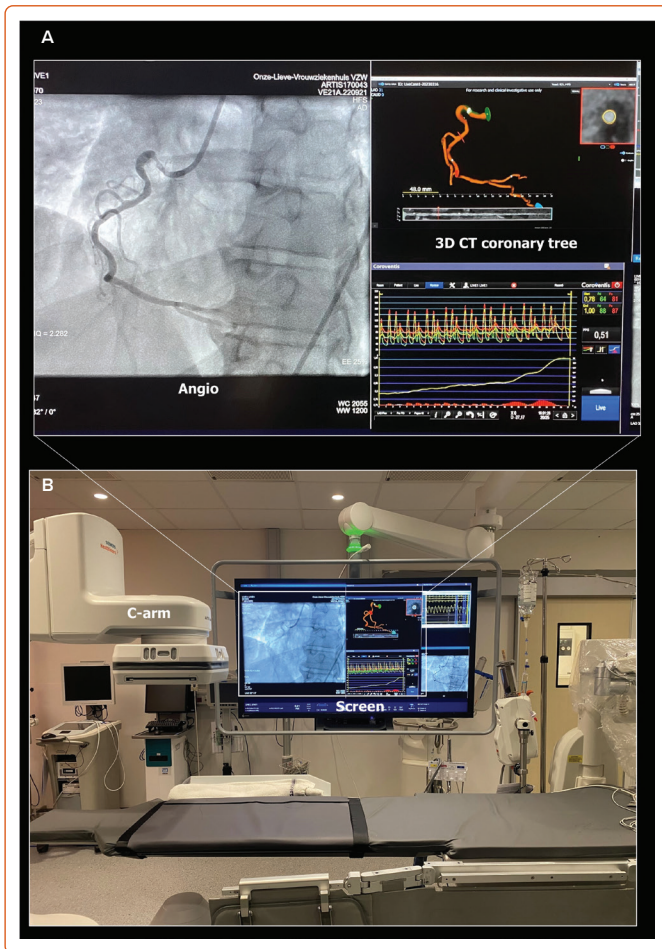
The FFR_{CT} Planner (HeartFlow) is a novel tool that predicts FFR in response to changes to patient-specific lumen geometry in real time. The FFR_{CT} Planner recalculates FFR after the virtual removal of coronary artery stenoses predicting post-PCI FFR. Post-PCI FFR is a metric of the degree of functional revascularisation and has been identified as an independent predictor of cardiac death and MI after PCI.⁴ Sonck et al. prospectively validated this tool showing high accuracy and precision with invasively measured post-PCI FFR as a reference.¹⁸ In addition, in cases of tandem lesions, FFR_{CT} is the most accurate tool to predict the interactions or cross-talk between lesions, outperforming even invasively derived algorithms. As with the FFR_{CT} technology, the FFR_{CT} Planner is powered by CFD. Several pre-computations are performed to understand the

relationship between flow and resistance in every vessel location. Planned lumen changes modify the expected flow rate through the vessels and are used with the geometry change to calculate a new FFR_{CT} along the vessel.¹⁹

Myocardial Mass at Risk

Vessel-specific myocardial mass can be quantified from the coronary CTA images using either the Voronoi's algorithm or CFD-based technique. These software programmes automatically provide the territory-specific myocardial mass.^{3,20-22} The information provided by the mass is used during the CFD simulations to estimate the amount of blood flow going through each of the coronary vessels. The estimation of blood flow is essential information to accurately calculate trans-lesional pressure gradients. In addition, the subtended myocardial mass has been associated with FFR and myocardial ischaemia.^{23,24} For PCI planning, myocardial mass information is of particular interest in the case of bifurcation lesions, when knowing the mass at risk of the side branch may help determine the PCI bifurcation strategy in terms of side branch protection or stenting. It should be underlined that the current process of mass analysis does not distinguish between viable and non-viable myocardium. Nonetheless, tissue characterisation by CT with the

Figure 3: Cath Lab Setup for Online CT Guidance



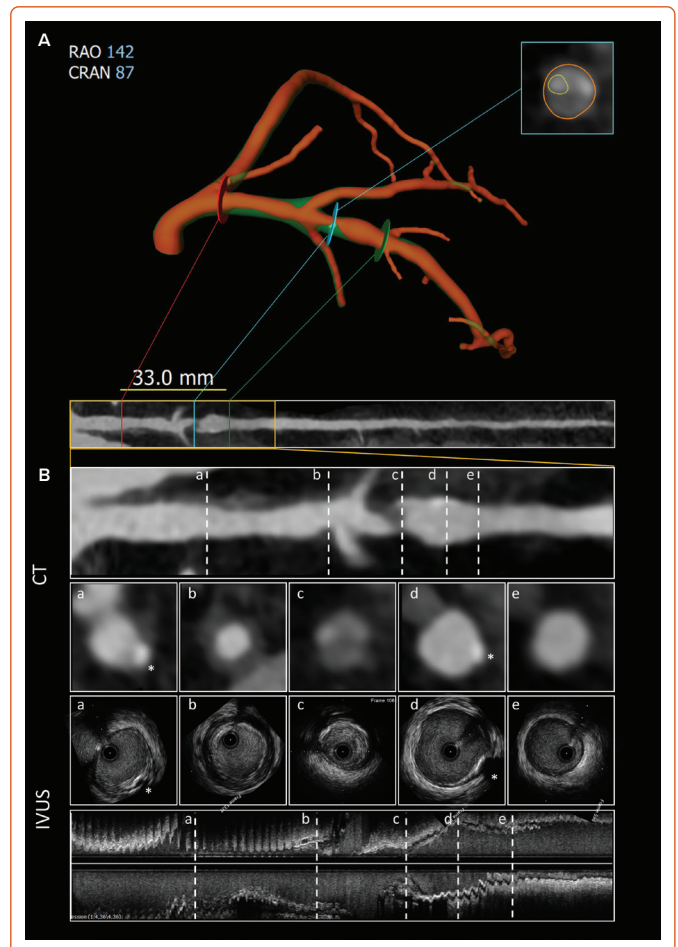
The cath lab setup comprises synchronisation hardware between the C-arm and CT software with the projection of the 3D CT-derived geometry projected alongside the angiographic image.

combination of CT perfusion allows a scar to be distinguished from healthy myocardium.²⁵

Cath Lab Setup Based on Coronary CT Angiography

The anatomical information on coronary anatomy and function obtained by coronary CTA helps to plan the procedure by selecting and preparing the material upfront and defining the PCI strategy. For example, adequate catheter support is critical for PCI, especially in complex disease. The evaluation of the coronary artery take-offs in the axial views from CTA assists in selecting the most appropriate guiding catheter. An anterior take-off of the ostial right coronary artery results in insufficient support from classical catheters (e.g. Judkins right) and makes one consider selecting an Amplatz left guiding catheter. Thus, by anticipating the most appropriate catheter, coronary CTA allows operators to save resources, contrast and procedural time, while avoiding catheter exchanges during the procedure. In addition, in other types of coronary anomalies and in bypass grafts, coronary CTA is the preferred imaging modality to locate the ostium of the vessels. Further studies are necessary to understand how to select the most appropriate catheter for each anatomy where cannulation simulations might be useful. Coronary CTA is useful for patients previously treated by coronary artery bypass grafting (CABG) and planned to undergo coronary angiography. The presence of CABG creates *per se* a complex scenario, as catheterisation of the bypass grafts can be challenging and time-consuming. Coronary CTA can define the number, ostium location, target

Figure 4: The Software of 3D CT-Derived Geometry for Cath Lab Integration

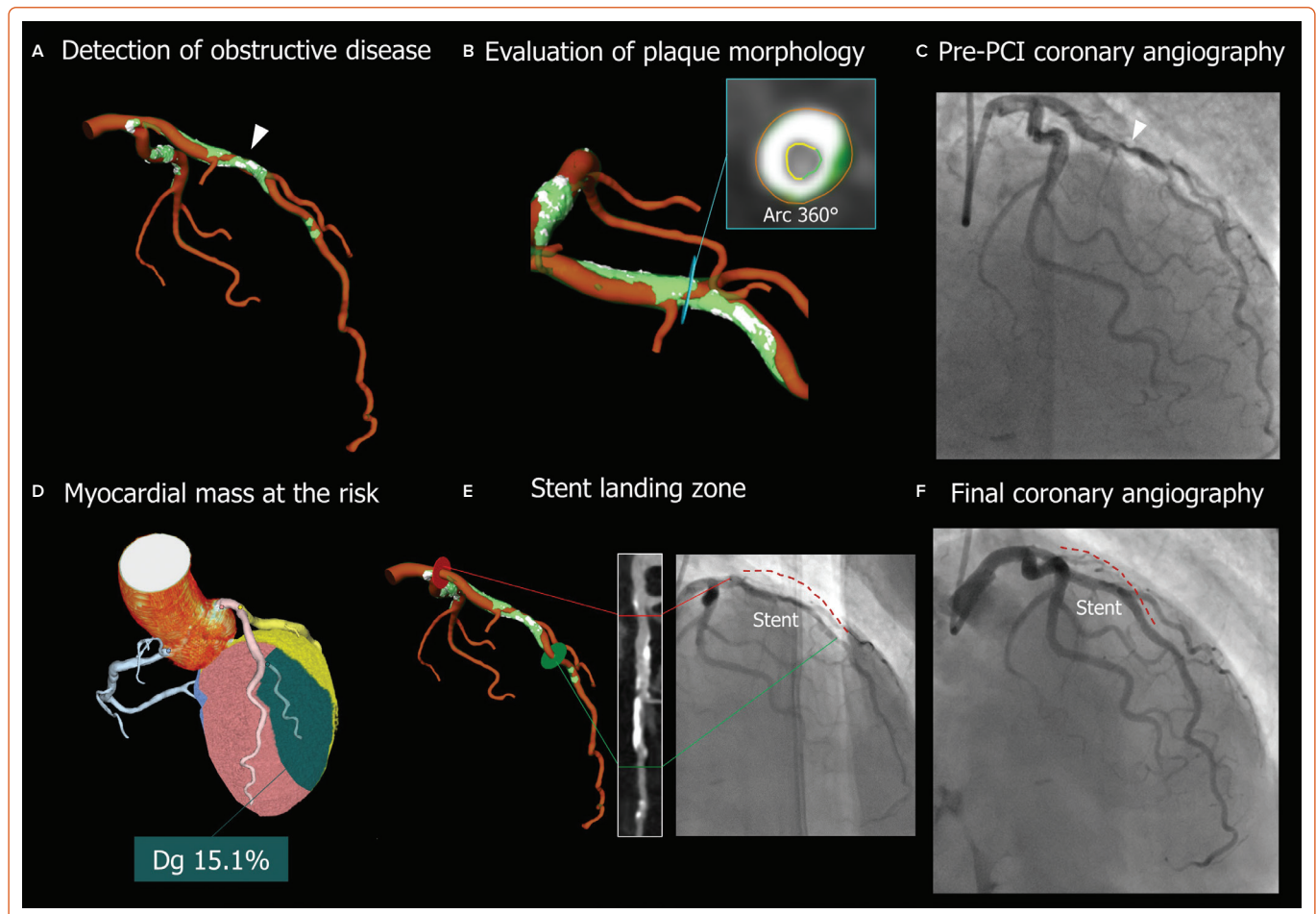


A: QAngioCT cath lab viewer. The centre image shows the 3D CT-derived geometry. The bottom image shows the straightened MPR. Red lines in 3D CT-derived coronary geometry and straightened MPR indicate the proximal stent landing position and green lines indicate the distal stent landing position. The expected stent length from the red line to the green line is 33.0 mm. The blue line shows the position of the MLA, which corresponds to cross-sections 'c' image; B: The matched the longitudinal and cross-sectional images between CT (top) and IVUS (bottom). The white asterisk denotes the calcification plaque. IVUS = intravascular ultrasound; MLA = minimum lumen area; MPR = multiplanar reconstruction.

native coronary and patency of the bypass grafts. Potential lesions on the bypass graft can also be visualised.²⁶ These findings are not only useful for material selection but may also impact arterial access. Recently, the BYPASS-CTCA study demonstrated that, in patients who had previously undergone CABG and were referred for an invasive coronary angiography, coronary CTA planning increased the use of radial access along with reducing procedural duration and complications while improving patients' satisfaction.²⁷ The case examples of beneficial information on the coronary anatomy obtained by coronary CTA are shown in Figure 2.

Coronary CTA can provide data on the entry cap (blunted or tapered), calcium severity, the presence of calcium at the entry and exit of the chronic total occlusion (CTO) and the presence of multiple occlusions, among other features. Clinical trials addressing the value of CT for CTO planning have shown that CT contributes to a higher success rate compared with no CT planning.^{28,29} There is the potential for artificial intelligence algorithms to – in addition to detecting stenosis and identifying plaque composition – also provide information about PCI planning.

Figure 5: Representative Cases of CT-Guided Percutaneous Coronary Intervention in Complex Lesion



A 72-year-old man with hypertension and diabetes presented with stable angina (CCS 3). Significant diffuse disease is present in the mid-LAD shown on coronary CTA evaluation. A: Detection of significant stenosis (white) in the LAD in 3D CT-derived geometry. 3D CT-derived coronary geometry allows us to easily identify a significant calcified plaque in the mid LAD. B: Evaluation of plaque morphology with the blue line denoting the cross-section with the MLA and concentric calcium plaque; C: ICA pre-PCI. ICA showed the significant diffuse disease in the middle LAD (white arrow); D: myocardial mass at risk. The software (Synapse Vincent, Fujifilm) showed that the myocardial mass at risk was 15.1% in diagonal branch; E: The lesion length considering complete coverage of the lesion (normal to normal) used for stent length selection. The red line denotes the proximal stent landing zone and the green line the distal stent landing zone. Accordingly, a 48 mm drug-eluting stent was implanted in this lesion based on online coronary CTA assessment; F: The final ICA. Dg = diagonal branch; CCS = Canadian Cardiovascular Society; CTA = CT angiography; ICA = invasive coronary angiography; LAD = left anterior descending artery; MLA = minimum lumen area; PCI = percutaneous coronary intervention.

Coronary Calcification

One of the main limitations of coronary CTA for diagnostic evaluation is the presence of calcium, which hampers luminal evaluation and frequently leads to an overestimation of disease severity. For PCI planning, the high sensitivity of CT for calcium represents a unique opportunity to determine the severity of calcifications. Patients with severe calcifications undergoing PCI have a significantly higher rate of target-vessel failure because of higher procedural risks and reduced stent durability.³⁰ Coronary CTA can provide a precise evaluation of the calcium burden, arc extension, thickness, length and distribution.³¹ However, it is relevant to mention that – at this stage – coronary CTA is unable to assess the location of calcium (superficial versus deep) and to differentiate nodular from other types of calcifications. Nonetheless, providing an accurate assessment of calcium arc and burden coronary CTA informs the necessity of plaque-modification techniques such as a cutting balloon, intravascular lithotripsy, rotational atherectomy (RA) and orbital atherectomy during the PCI. Recent observational reports have demonstrated an association between calcium characteristics and the need for RA.^{32,33} Sekimoto et al. showed that calcium score and arc are associated with the need for RA during PCI, and recently Kurogi et al. reported that the mean density of the cross-sectional CT image, potentially representing information about calcific strength, is the

strongest predictor of the need for RA during PCI.^{32,33} Therefore, the application of artificial intelligence for the accurate segmentation of calcific plaques, with the potential for a more detailed stratification of calcific plaque, is a promising field. In the future, coronary CTA-based algorithms will likely be used to determine the necessity of calcific plaque modification with dedicated devices.³⁴

Online Percutaneous Coronary Intervention Guidance

Coronary CTA is now being tested as a tool to guide PCI; this approach provides the possibility of assessing plaque extension and distribution during invasive coronary angiography. The coronary tree with 3D reconstructions of the plaque in the three vessels is projected onto the screen in the cath lab during the procedure, alongside the invasive coronary angiography (QAngioCT Cath Lab, Medis Medical Imaging Systems; Figure 3). The 3D coronary tree model is synchronised in real-time to the C-arm position to match the views with the fluoroscopic arm and continuously visualised following changes in angiographic projections (Supplementary Video 1). This approach enables finding the optimal view without contrast injection or radiation. Moreover, it facilitates the interpretation and distinction of plaque components, as they are colour-coded according to their Hounsfield units.

PCI guidance using coronary CTA starts with the identification of significant obstructive disease and the evaluation of plaque characteristics and disease extension. The additional benefit of coronary CTA is that it provides a 3D depiction of the complete tree with atherosclerotic plaque characterisation, similar to intravascular imaging (Figure 4). Thus, by simultaneously displaying the plaque in 3D, the coronary CTA overcomes one of the main drawbacks of the angiogram, which shows only the lumen. This additional information provides a complete depiction of the disease and plaque types and assists in stent deployment.³⁵ Moreover, it allows for real-time measurements to adjust the PCI strategy. While the current approach relies on semi-automatic segmentation of the coronary tree, future iteration based on artificial intelligence will allow for rapid reconstruction and plaque characterisation with treatment recommendations based on the patient's specific disease. A case example of CT-guided PCI is shown in Figure 5.

Conclusion

Leveraging artificial intelligence, the reconstruction process will be fully automated, providing reproducible and comprehensive coronary CTA assessments for PCI planning that will be likely to influence outcomes, resulting in a cost-saving approach.³⁶ Deep learning using large amounts of data has the potential to improve speed, diagnostic performance and image analysis of coronary CTA by providing automated and objective results. The integration of coronary CTA inside the cath lab is a novel approach to CAD diagnosis and treatment. CT-guided PCI has the potential to increase the use of imaging-guided PCI. The ongoing P4 clinical trial (NCT05253677) is currently investigating whether a CT-guided PCI approach results in similar outcomes compared with intravascular ultrasound-guided PCI. Coronary CTA could likely become the predominant imaging modality for PCI guidance. □

- Andreini D, Magnoni M, Conte E, et al. Coronary plaque features on CTA can identify patients at increased risk of cardiovascular events. *JACC Cardiovasc Imaging* 2020;13:1704–17. <https://doi.org/10.1016/j.jcmg.2019.06.019>; PMID: 31422137.
- Knuuti J, Wijns W, Saraste A, et al. 2019 ESC guidelines for the diagnosis and management of chronic coronary syndromes. *Eur Heart J* 2020;41:407–77. <https://doi.org/10.1093/eurheartj/ehz425>; PMID: 31504439.
- Taylor CA, Fonte TA, Min JK. Computational fluid dynamics applied to cardiac computed tomography for noninvasive quantification of fractional flow reserve: scientific basis. *J Am Coll Cardiol* 2013;61:2233–41. <https://doi.org/10.1016/j.jacc.2012.11.083>; PMID: 23562923.
- Hwang D, Koo BK, Zhang J, et al. Prognostic implications of fractional flow reserve after coronary stenting: a systematic review and meta-analysis. *JAMA Netw Open* 2022;5:e2232842. <https://doi.org/10.1001/jamanetworkopen.2022.32842>; PMID: 36136329.
- Andreini D, Pontone G, Mushtaq S, et al. A long-term prognostic value of coronary CT angiography in suspected coronary artery disease. *JACC Cardiovasc Imaging* 2012;5:690–701. <https://doi.org/10.1016/j.jcmg.2012.03.009>; PMID: 22789937.
- Dai N, Chen Z, Zhou F, et al. Coronary CT angiography-derived plaque characteristics and physiologic patterns for peri-procedural myocardial infarction and subsequent events. *Eur Heart J Cardiovasc Imaging*. 2023;24:897–908. <https://doi.org/10.1093/ehjci/jead025>; PMID: 36808235.
- Nakazawa G, Tanabe K, Onuma Y, et al. Efficacy of culprit plaque assessment by 64-slice multidetector computed tomography to predict transient no-reflow phenomenon during percutaneous coronary intervention. *Am Heart J* 2008;155:1150–7. <https://doi.org/10.1016/j.ahj.2008.01.006>; PMID: 18513532.
- Uetani T, Amano T, Kunimura A, et al. The association between plaque characterization by CT angiography and post-procedural myocardial infarction in patients with elective stent implantation. *JACC Cardiovasc Imaging* 2010;3:19–28. <https://doi.org/10.1016/j.jcmg.2009.09.016>; PMID: 20129526.
- Williams MC, Kwiecinski J, Doris M, et al. Low-attenuation noncalcified plaque on coronary computed tomography angiography predicts myocardial infarction: results from the multicenter SCOT-HEART trial (Scottish Computed Tomography of the HEART). *Circulation* 2020;141:1452–62. <https://doi.org/10.1161/CIRCULATIONAHA.119.044720>; PMID: 32174130.
- Lin A, Manral N, McElhinney P, et al. Deep learning-enabled coronary CT angiography for plaque and stenosis quantification and cardiac risk prediction: an international multicentre study. *Lancet Digit Health* 2022;4:e256–65; [https://doi.org/10.1016/S2589-7500\(22\)00022-X](https://doi.org/10.1016/S2589-7500(22)00022-X); PMID: 35337643.
- Dey D, Slomka PJ, Leeson P, et al. Artificial intelligence in cardiovascular imaging: JACC state-of-the-art review. *J Am Coll Cardiol* 2019;73:1317–35. <https://doi.org/10.1016/j.jacc.2018.12.054>; PMID: 30898208.
- Norgaard BL, Leipsic J, Gaur S, et al. Diagnostic performance of noninvasive fractional flow reserve derived from coronary computed tomography angiography in suspected coronary artery disease: the NXT trial (Analysis of Coronary Blood Flow Using CT Angiography: Next Steps). *J Am Coll Cardiol* 2014;63:1145–55. <https://doi.org/10.1016/j.jacc.2013.11.043>; PMID: 24486266.
- Norgaard BL, Fairbairn TA, Safian RD, et al. Coronary CT angiography-derived fractional flow reserve testing in patients with stable coronary artery disease: recommendations on interpretation and reporting. *Radiol Cardiothorac Imaging* 2019;1:e190050. <https://doi.org/10.1148/ryct.2019190050>; PMID: 33778528.
- Lee JM, Choi G, Koo BK, et al. Identification of high-risk plaques destined to cause acute coronary syndrome using coronary computed tomographic angiography and computational fluid dynamics. *JACC Cardiovasc Imaging* 2019;12:1032–43. <https://doi.org/10.1016/j.jcmg.2018.01.023>; PMID: 29550316.
- Piroth Z, Toth GG, Tonino PAL, et al. Prognostic value of fractional flow reserve measured immediately after drug-eluting stent implantation. *Circ Cardiovasc Interv* 2017;10:e005233. <https://doi.org/10.1161/CIRCINTERVENTIONS.116.005233>; PMID: 28790165.
- Collet C, Collison D, Mizukami T, et al. Differential improvement in angina and health-related quality of life after PCI in focal and diffuse coronary artery disease. *JACC Cardiovasc Interv* 2022;15:2506–18. <https://doi.org/10.1016/j.jcin.2022.09.048>; PMID: 36543445.
- Takagi H, Leipsic JA, McNamara N, et al. Trans-lesional fractional flow reserve gradient as derived from coronary CT improves patient management: ADVANCE registry. *J Cardiovasc Comput Tomogr* 2022;16:19–26. <https://doi.org/10.1016/j.jcct.2021.08.003>; PMID: 34518113.
- Sonck J, Nagumo S, Norgaard BL, et al. Clinical validation of a virtual planner for coronary interventions based on coronary CT angiography. *JACC Cardiovasc Imaging* 2022;15:1242–55. <https://doi.org/10.1016/j.jcmg.2022.02.003>; PMID: 35798401.
- Sankaran S, Lesage D, Tombropoulos R, et al. Physics driven real-time blood flow simulations. *Comput Methods Appl Mech Eng* 2020;364:112963. <https://doi.org/10.1016/j.cma.2020.112963>.
- Guibas L, Stolfi J. Primitives for the manipulation of general subdivisions and the computation of Voronoi. *ACM Trans Graph* 1985;4:74–123. <https://doi.org/10.1145/282918.282923>.
- Ide S, Sumitsuiji S, Yamaguchi O, Sakata Y. Cardiac computed tomography-derived myocardial mass at risk using the Voronoi-based segmentation algorithm: a histological validation study. *J Cardiovasc Comput Tomogr* 2017;11:179–82. <https://doi.org/10.1016/j.jcct.2017.04.007>; PMID: 28431861.
- Taylor CA, Gaur S, Leipsic J, et al. Effect of the ratio of coronary arterial lumen volume to left ventricle myocardial mass derived from coronary CT angiography on fractional flow reserve. *J Cardiovasc Comput Tomogr* 2017;11:429–36. <https://doi.org/10.1016/j.jcct.2017.08.001>; PMID: 28789941.
- Kim CH, Yang S, Zhang J, et al. Differences in plaque characteristics and myocardial mass: implications for physiological significance. *JACC Asia* 2022;2:157–67. <https://doi.org/10.1016/j.jacasi.2021.11.011>; PMID: 36339124.
- Yang DH, Kang SJ, Koo HJ, et al. Incremental value of subtended myocardial mass for identifying FFR-verified ischemia using quantitative CT angiography: comparison with quantitative coronary angiography and CT-FFR. *JACC Cardiovasc Imaging* 2019;12:707–17. <https://doi.org/10.1016/j.jcmg.2017.10.027>; PMID: 29361491.
- van Driest FY, van der Geest RJ, Broersen A, et al. Quantification of myocardial ischemia and subtended myocardial mass at adenosine stress cardiac computed tomography: a feasibility study. *Int J Cardiovasc Imaging* 2021;37:3313–22. <https://doi.org/10.1007/s10554-021-02314-z>; PMID: 34160721.
- Barbero U, Iannaccone M, d'Ascenzo F, et al. 64 slice-coronary computed tomography sensitivity and specificity in the evaluation of coronary artery bypass graft stenosis: A meta-analysis. *Int J Cardiol* 2016;216:52–7. <https://doi.org/10.1016/j.ijcard.2016.04.156>; PMID: 27140337.
- Beirne AM, Rathod KS, Castle E, et al. The BYPASS-CTCA study: the value of computed tomography cardiac angiography (CTCA) in improving patient-related outcomes in patients with previous bypass operation undergoing invasive coronary angiography: study protocol of a randomised controlled trial. *Ann Transl Med* 2021;9:1395. <https://doi.org/10.21037/atm-21-1455>; PMID: 34733947.
- Opolski MP, Achenbach S. CT Angiography for revascularization of CTO: crossing the borders of diagnosis and treatment. *JACC Cardiovasc Imaging* 2015;8:846–58. <https://doi.org/10.1016/j.jcmg.2015.05.001>; PMID: 26183556.
- Hong SJ, Kim BK, Cho I, et al. Effect of coronary CTA on chronic total occlusion percutaneous coronary intervention: a randomized trial. *JACC Cardiovasc Imaging* 2021;14:1993–2004. <https://doi.org/10.1016/j.jcmg.2021.04.013>; PMID: 34147439.
- Huisman J, van der Heijden LC, Kok MM, et al. Impact of severe lesion calcification on clinical outcome of patients with stable angina, treated with newer generation permanent polymer-coated drug-eluting stents: a patient-level pooled analysis from TWENTE and DUTCH PEERS (Twente II). *Am Heart J* 2016;175:121–9. <https://doi.org/10.1016/j.ahj.2016.02.012>; PMID: 27179731.
- Monizzi G, Sonck J, Nagumo S, et al. Quantification of calcium burden by coronary CT angiography compared to optical coherence tomography. *Int J Cardiovasc Imaging* 2020;36:2393–402. <https://doi.org/10.1007/s10554-020-01839-z>; PMID: 33205340.
- Kurogi K, Ishii M, Nagatomo T, et al. Mean density of computed tomography for predicting rotational atherectomy during percutaneous coronary intervention. *J Cardiovasc Comput Tomogr* 2023;17:120–9. <https://doi.org/10.1016/j.jcct.2023.02.002>; PMID: 36775780.
- Sekimoto T, Akutsu Y, Hamazaki Y, et al. Regional calcified plaque score evaluated by multidetector computed tomography for predicting the addition of rotational atherectomy during percutaneous coronary intervention. *J Cardiovasc Comput Tomogr* 2016;10:221–8. <https://doi.org/10.1016/j.jcct.2016.01.004>; PMID: 26811266.
- Petersen K, Schaap M, Mirza S, et al. Quantitative assessment of AI-based CCTA plaque volume compared with IVUS. *J Cardiovasc Comput Tomogr* 2022;16(4 Suppl 24):452. <https://doi.org/10.1016/j.jcct.2022.06.057>.
- Ali Z, Landmesser U, Karimi Galoughi K, et al. Optical coherence tomography-guided coronary stent implantation compared to angiography: a multicentre randomised trial in PCI - design and rationale of ILUMIEN IV: Optimal PCI. *EuroIntervention* 2021;16:1092–9. <https://doi.org/10.4244/EIJ-D-20-00501>; PMID: 32863246.
- Serruys PW, Chichareon P, Modolo R, et al. The SYNTAX score on its way out or... towards artificial intelligence: part II. *EuroIntervention* 2020;16:60–75. <https://doi.org/10.4244/EIJ-D-19-00543B>; PMID: 31651398.